NUMERICAL AND EXPERIMENTAL INVESTIGATION OF ROCKING STABILITY OF RIGID BLOCKS DURING SINGLE SINE-WAVE EXCITATION

Nina Čeh* – Gordan Jelenić

University of Rijeka, Faculty of Civil Engineering, Radmile Matejčić 3, 51000 Rijeka

ARTICLE INFO

***Article history*:**
Received: 16.02.2022.
Received in revised form: 27.05.2022.
Accepted: 11.07.2022.

Keywords:
Rocking stability
Restitution coefficient
Single-wave harmonic excitation
Overturning
Experimental benchmark

DOI: https://doi.org/10.30765/er.1950

Abstract:

Rocking stability of a rigid prismatic block standing on a rigid base subject to a simple harmonic acceleration function is still an important dynamics problem, in which energy loss is often not treated accurately enough. The energy loss at impacts during rocking is here examined. The stability for various slendernesses and sizes of a rocking block is assessed numerically, where an improved coefficient capable of estimating the size effect is considered. A number of relevant cases are validated experimentally, with a specially designed set of well-controlled and documented rocking benchmark tests on a shaking table system.

1 Introduction

Rocking is an important mode of motion in many historic structures [1], but also in various structural elements in modern industrial complexes (ex. masonry structures after the failure of the binder or blocks in AGR nuclear power plants) [2] subject to dynamic excitation such as earthquake. There is also a rising interest in utilizing rocking as a means for seismic isolation of tall slender buildings [1]. For these reasons, it is important to determine whether a body subject to an excitation will rock (and finally settle due to energy dissipation) or will overturn.

In-plane rocking of rigid prismatic blocks was first addressed by Housner in 1963 [3]. He derived the nonlinear equation of motion of the block standing on a rigid base with a single degree of freedom - the angle of rotation. He assumed that for slender blocks a linearized equation of motion is appropriate and derived the analytical solutions for what he called the 'period and frequency of rocking motion', which turned out to be dependent on the amplitude of rocking. Following Housner's work, the analytical condition for initiation of rocking and the minimum ground acceleration of a specific acceleration function necessary to overturn a block have been further derived from the linearized equation of motion [3]–[7], while the fully nonlinear equation of motion using the state-space procedure and built-in ODE solvers has been addressed in [5], [6], [8]–[11]. In an attempt to characterise rocking motion more completely, transient and steady-state dynamic response of a single rigid block due to earthquakes [7], random-noise excitations [12] and pulse-type excitations [9] have been investigated.

However, rocking of a single block due to a simple harmonic function, such as a single sine or cosine wave, is still not characterised in the sense that the real energy-loss during rocking is taken into account via the appropriate coefficient of restitution. Many researchers [13]–[21] concluded that the experimentally obtained results for dynamic response and overturning of blocks due to base acceleration cannot be described using the classical Housner's approach, since the energy loss during impacts he described does not model the real behaviour well enough. For this reason, here we analyse the stability of a block during simple harmonic ground acceleration function numerically and validate the results experimentally. The improved estimate of the restitution coefficient, introduced independently by Kalliontzis et al. [22] and by Chatzis et al. [23], is employed. The improved estimate, which is derived from the assumption that the resultant impulse at the time

* Corresponding author
E-mail address: nina.ceh@uniri.hr

of impact acts at some other point than the corner of the block, proves to be a better approximation of the real restitution [24] than the widely used Housner's restitution [3].

The improved estimate of the restitution coefficient has previously been addressed in [22] for block excited with functions based on real earthquake motions, while the effect of the uncertainty of the position of the impact impulse to the rocking stability due to sine- and cosine-wave excitation is addressed in [23]. The rocking block problem is still an interesting case, since it presents an important mode of motion of multi-block structures (such as masonry and dry-stone structures) and coupled structures (such as quasi-rigid element near a deformable structure). The energy loss mechanism is still often described only by Housner's restitution [25]–[27] (among others), so this work aims to raise the importance of taking the improved coefficient of restitution into account, since it results in safer overturning conditions [28], [29]. Thus, the objective here is to numerically and experimentally derive safer conditions under which a block overturns when subjected to a single sine-wave or cosine-wave acceleration, than those available in the literature [1], considering the improved estimate of the coefficient of restitution obtained experimentally [24].

2 Problem description

2.1 Equations of motion and numerical algorithm

Rocking of a single rigid prismatic block due to an arbitrary horizontal base acceleration function is described by the following equations of motion [3]

$$I_A\ddot{\theta} + mgR\sin(\alpha-\theta) + m\ddot{u}R\cos(\alpha-\theta) = 0 \quad \text{if} \quad \theta > 0 \tag{1}$$

$$I_A\ddot{\theta} - mgR\sin(\alpha+\theta) + m\ddot{u}R\cos(\alpha+\theta) = 0 \quad \text{if} \quad \theta < 0, \tag{2}$$

where θ is the angle of rotation, m is the mass of the block, $I_A = 4/3mR^2$ is its moment of inertia around either of the corners, $\alpha = \tan^{-1} h/b$ is its angle of slenderness, h is the height and b is the width of the block, $R = 1/2\sqrt{b^2+h^2}$, g is the gravitational constant, $\ddot{u}$ is the ground acceleration function, while the superimposed dots indicate time differentiation. Figure 2 shows free-body and mass-acceleration diagrams for $\theta > 0$.

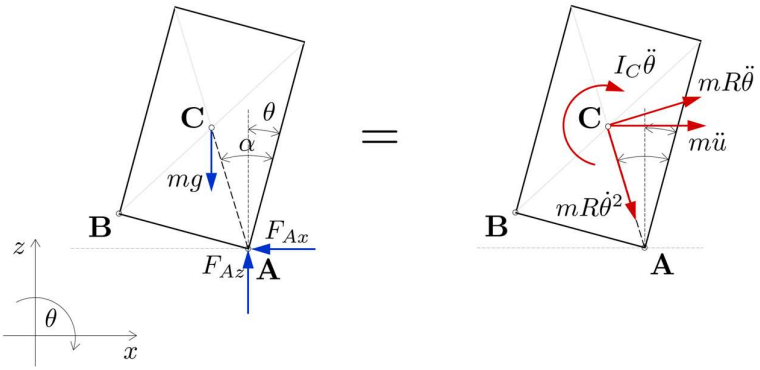

Figure 1. Free-body and mass-acceleration diagrams during rotation around contact point A (F_{Ax} and F_{Ay} are the contact reactions).

Equation (1) can be linearised if we limit our research to only slender blocks with small rotations. However, in order to describe rocking of blocks with arbitrary slenderness which can undergo large rotations, it is necessary to use the fully nonlinear equation of motion. In this work, rocking and overturning due to two simple harmonic acceleration excitations - a single sine wave and a single cosine wave (see Figure 2) - is examined. The acceleration function is described with its amplitude a_0 and angular frequency $\omega = 2\pi/t_b$, where t_b is the period of excitation.

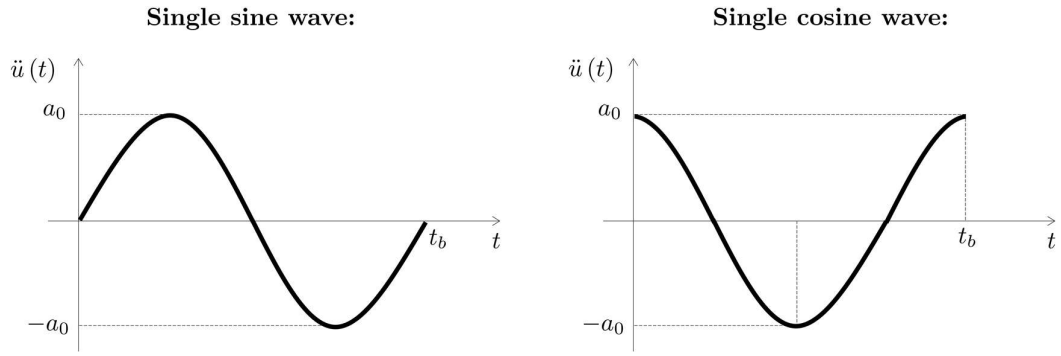

Figure 2. Ground acceleration functions examined.

2.2 Numerical integration

Equations (1) and (2) with acceleration function $\ddot{u}$ as shown in Figure 2 are now solved numerically using the well-known Newmark's trapezoidal rule [30]:

$$\dot{\theta}_{n+1} = \frac{2}{\Delta t}(\theta_{n+1} - \theta_n) - \dot{\theta}_n \,, \tag{3}$$

$$\ddot{\theta}_{n+1} = \frac{4}{\Delta t^2}(\theta_{n+1} - \theta_n) - \frac{4}{\Delta t}\dot{\theta}_n - \ddot{\theta}_n \,, \tag{4}$$

where Δt is the time-step length, leading to:

$$\frac{4}{\Delta t^2}(\theta_{n+1} - \theta_n) - \frac{4}{\Delta t}\dot{\theta}_n - \ddot{\theta}_n + p^2 \sin(\alpha - \theta_{n+1}) + \frac{p^2}{g}\ddot{u}_{n+1}\cos(\alpha - \theta_{n+1}) = 0 \quad \text{if} \quad \theta_n, \theta_{n+1} > 0 \tag{5}$$

$$\frac{4}{\Delta t^2}(\theta_{n+1} - \theta_n) - \frac{4}{\Delta t}\dot{\theta}_n - \ddot{\theta}_n - p^2 \sin(\alpha + \theta_{n+1}) + \frac{p^2}{g}\ddot{u}_{n+1}\cos(\alpha + \theta_{n+1}) = 0 \quad \text{if} \quad \theta_n, \theta_{n+1} < 0, \tag{6}$$

where $p = \sqrt{3g/4R}$ is the so-called frequency parameter.

At each time-step, the nonlinear equation is solved iteratively using the Newton-Raphson iterative procedure. An impact detection procedure described in [24] is built into the numerical algorithm used here. When at a time t_{n+1} either $\theta_n > 0$ and $\theta_{n+1} < 0$ or $\theta_n < 0$ and $\theta_{n+1} > 0$ occurs, the dynamic equilibrium for this time step is repeated for an *unknown time-step length* $\Delta t'$ rather than θ_{n+1}, under the conditions that $\theta_{n+1} \coloneqq 0$.

The pre-impact angular velocity $\dot{\theta}^-$ and angular acceleration $\ddot{\theta}^-$ are then calculated as

$$\dot{\theta}^- = \frac{2}{\Delta t'}(0 - \theta_n) - \dot{\theta}_n \tag{7}$$

$$\ddot{\theta}^- = \frac{4}{\Delta t'^2}(0 - \theta_n) - \frac{4}{\Delta t'}\dot{\theta}_n - \ddot{\theta}_n \,, \tag{8}$$

the original time-step length Δt is restored and the time-stepping procedure switches to the next step and to the other equation of motion. At this point, however, the angular velocity at the beginning of the first post-impact time step has to be reduced considering appropriate restitution model.

2.3 Restitution model

Two restitution descriptions are compared in this study, where the restitution coefficient is defined as the ratio between the post-impact and pre-impact angular velocities. The classical Housner's model [3], which assumes that the contact impulse during impact takes place at the very edge of the block, defines the restitution coefficient as

$$\eta_H = 1 - \frac{3}{2}\sin^2\alpha \tag{9}$$

The modified restitution description, independently proposed by Kalliontzis's at al. [22] and Chatzis et al. [23], considers the fact that the contact impulse may act at any point between the edges of the block. The resulting restitution coefficient is defined as

$$\eta_M = \frac{4 - 3\sin^2\alpha\,(1+k^2)}{4 - 3\sin^2\alpha\,(1-k^2)} \tag{10}$$

The above equation follows the work by Kalliontzis et al. [22], where $k = \frac{\bar{b}}{b/2}$, and $\bar{b}$ is the distance of the point at which the contact impulse acts from the midpoint of the bottom side of the block, as shown in Figure 3.

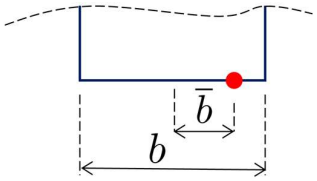

Figure 3. Impact position for calculating k needed in equation (10).

The two restitution formulas become increasingly similar with the increase in block's slenderness, but in general η_H significantly overestimates block's stability [24]. On the other hand, η_M involves an additional parameter, for which a method to determine it has to be devised.

2.4 Rocking stability

Stability of the block is characterised based on whether the block overturns or rocks in a stable fashion (and finally settles) during the excitation or after it drops to zero. Rocking stability is assessed using the described numerical procedure based on the nonlinear equation of motion by running the algorithm multiple times for different excitation frequencies and amplitudes and documenting the outcome in the frequency-amplitude space. In this way the areas with the excitation conditions under which overturning occurs and those under which rocking in stable fashion occurs are obtained.

The boundary between these areas in the case of sine-wave acceleration is presented in Figures 4 and 5 for two slenderness ratios using both restitution formulas (with $k = 0.75$ in case of η_M, taken to outline the realistic variations of this coefficient, as shown in [22]). The values b have not been declared because these plots with normalized values on both horizontal and vertical axes should be valid for any value b if the size effect is not taken into consideration. The results in Figures 4 and 5 and in the rest of the paper are presented in terms of the normalised angular frequency $\frac{\omega}{p}$ on the horizontal axis and the normalised acceleration amplitude $\frac{a_0}{\mathrm{g}\tan\alpha}$ on the vertical axis. These figures stress the importance of the improved restitution estimate η_M, as it is clear that η_H may seriously overestimate a block's stability against overturning.

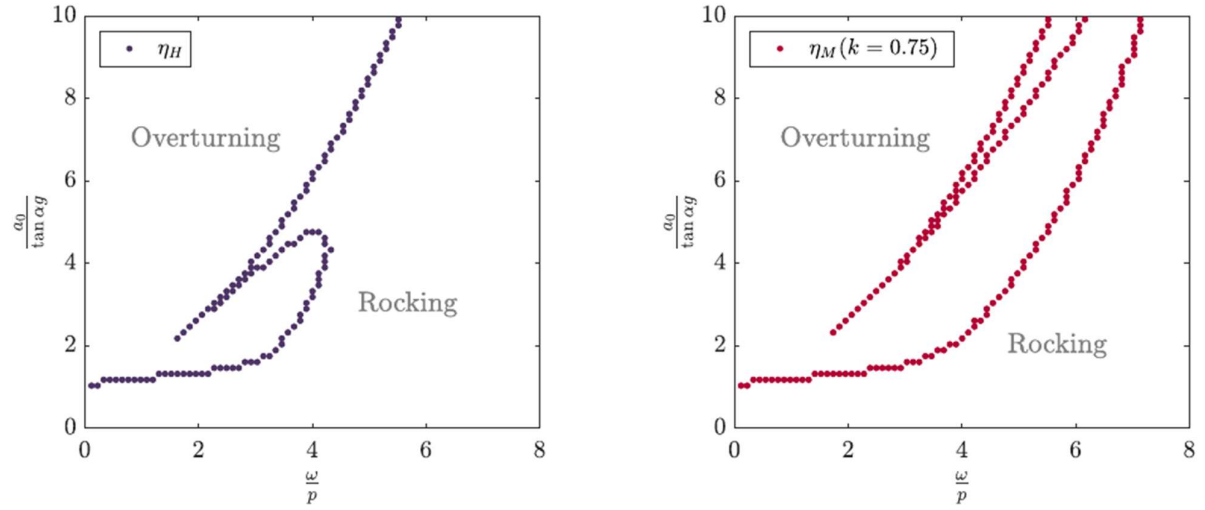

Figure 4. Stability graph due to a single sine wave for blocks with $\frac{h}{b} = 2.25$.

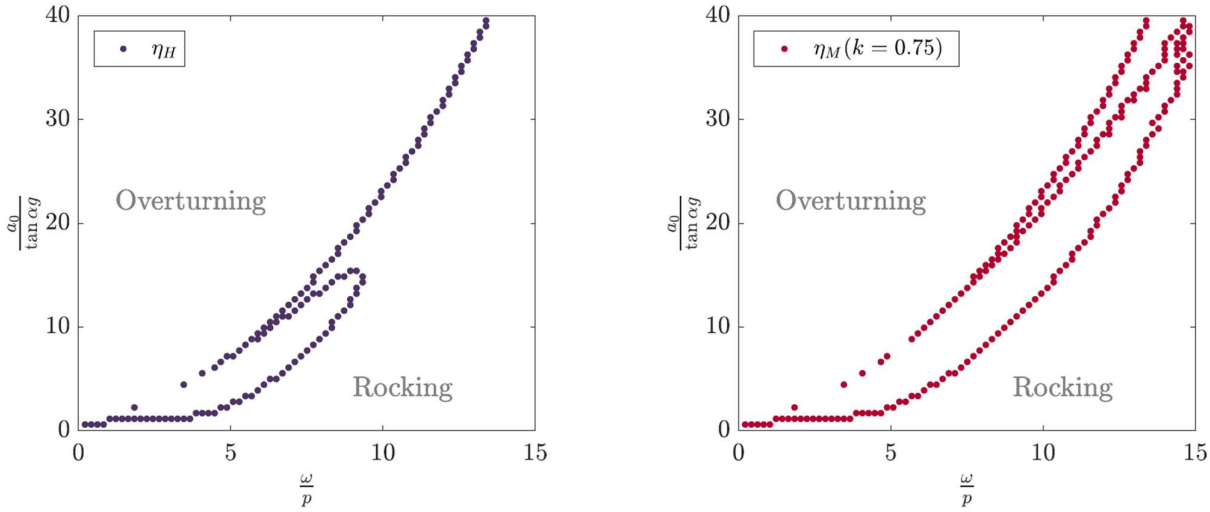

Figure 5. Stability graph due to a single sine wave for blocks with $\frac{h}{b} = 4.5$.

3 Rocking stability using an improved restitution estimate

Here we try to characterise the rocking more precisely using an estimate for k in equation (10) obtained from the series of free rocking experiments reported in [24].

3.1 Geometry

Stability of the blocks of two different slenderness ratios and two different sizes are examined here so that both the slenderness effect and the size effect may be investigated. The properties and the corresponding Housner's

restitution coefficients of the four blocks examined in this study are shown in Table 1, where the thickness of the blocks is equal to their width b. The actual denotation used for the blocks follows that introduced in [24]

Table 1. Geometry, η_H, and η_M for the analysed blocks.

Block	$m\ [g]$	$b\ [mm]$	$h\ [mm]$	$\frac{h}{b}$	$\alpha\ [rad]$	$R\ [mm]$	p	η_H	η_M
B3M	544.4	45	101.25	2.25	0.4182	55.4	11.524	0.7526	0.8106
B6M	1089.6	45	202.5	4.5	0.2187	103.7	8.423	0.9294	0.9472
B3L	1284.3	60	135	2.25	0.4182	73.9	9.978	0.7526	0.8598
B6L	2569.2	60	270	4.5	0.2187	138.3	7.294	0.9294	0.9617

For the blocks in Table 1 the unknown parameter k necessary to calculate η_M in (10) is obtained in [24] as $\mathrm{k} = 0.8608$ for a set of nine medium-sized blocks ($\mathrm{b} = 0.045$ m) with slenderness ranging from $\frac{h}{b} = 1.5$ to $\frac{h}{b} = 9.75$ and $\mathrm{k} = 0.7306$ for the corresponding set of large blocks ($\mathrm{b} = 0.06$ m), obtained as average values. The corresponding η_M are shown in Table 1.

3.2 Single sine-wave acceleration

Rocking stability and overturning conditions for a rigid block due to a single sine-wave acceleration excitation highly depend on the restitution coefficient. The overturning condition obtained from the numerical procedure described earlier using $\Delta\mathrm{t} = 0.001$ s and the Newton-Raphson convergence norm $1 \cdot 10^{-9}$ for the blocks and the corresponding restitution coefficients given in Table 1 are shown in Figures 6 and 7 for the blocks with slenderness ratio $\frac{h}{b}$ of 2.25 and 4.5, respectively.

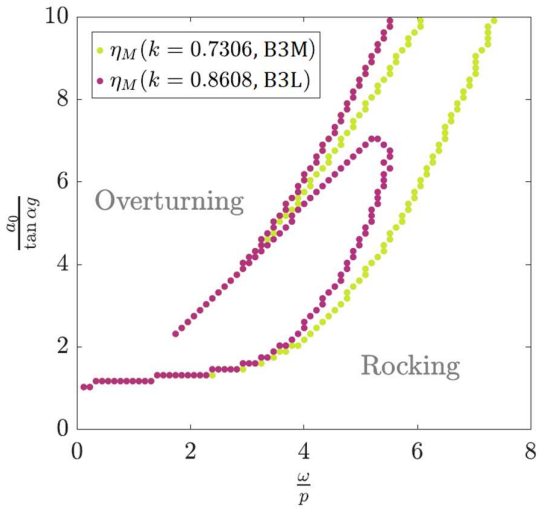

Figure 6. Stability graph for a single sine wave acceleration excitation for blocks with $\frac{h}{b} = 2.25$: B3M and B3L.

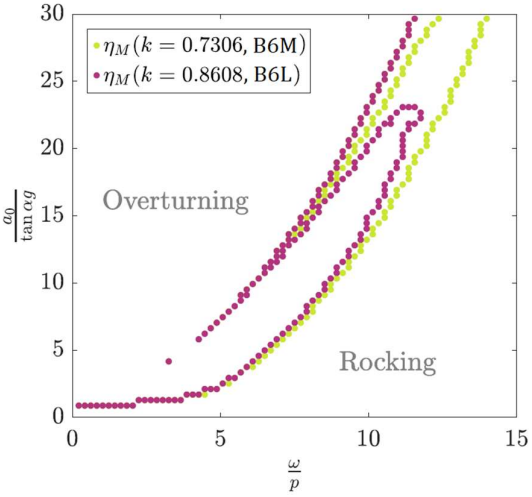

Figure 7. Stability graph for a single sine wave acceleration excitation for blocks with $\frac{h}{b} = 4.5$*: B6M and B6L.*

3.3 Single cosine-wave acceleration

The overturning conditions for a rigid block due to a single cosine-wave excitation acceleration obtained from the described numerical procedure vary only slightly with variation in block's size. Also, the overturning conditions are not strongly dependent of the restitution coefficient, which can be seen in Figures 8 and 9 for the blocks with slenderness ratio $\frac{h}{b}$ of 2.25 and 4.5, respectively.

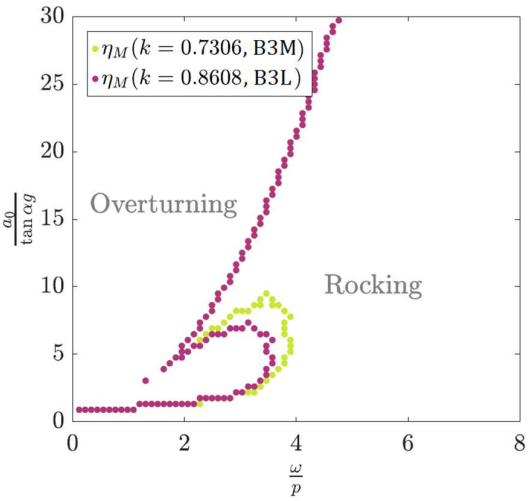

Figure 8. Stability graph for a single cosine wave acceleration excitation for blocks with $\frac{h}{b} = 2.25$*: B3M and B3L.*

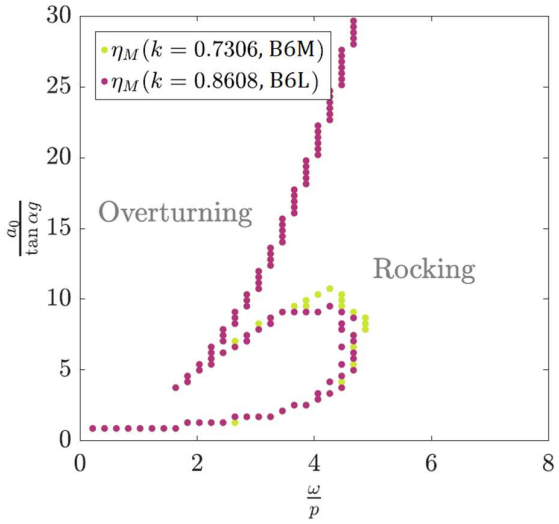

Figure 9. Stability graph for a single cosine wave acceleration excitation for blocks with $\frac{h}{b} = 4.5$: B6M and B6L.

4 Experimental set-up

4.1 Contact conditions in the model

In order to avoid slipping and bouncing and to assure only rocking motion, a specially designed system of tapes described in [24] is also used here (see Figure 10).

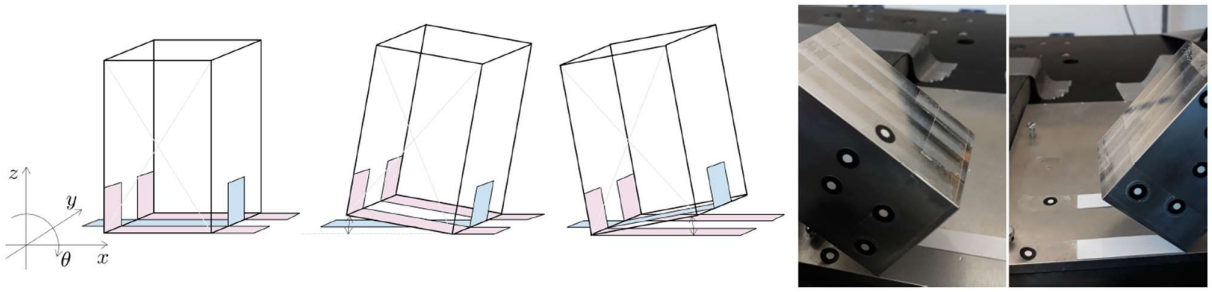

Figure 10. System of tapes designed to avoid sliding and jumping of the block.

4.2 Excitation and shaking table capacities

The excitation is experimentally performed by means of a biaxial shaking table Quanser ST-III run by a LabWiev-based software, which controls the position of the table. The conducted experiments are uniaxial. The desired acceleration excitation function, which is a part of the equation of motion in the simulations, should be integrated twice to get the position excitation function and as such given to the shaking table for the experimental tests. Due to the inertia of the table itself, the initial velocity of the system can only be equal to zero and rise gradually after that. For this reason, we can experimentally simulate either a cosine-wave acceleration excitation $\ddot{u}(\mathrm{t}) = \mathrm{a}_0 \cos(\omega\,\mathrm{t})$ leading to

$$\begin{aligned} \dot{u}(t) &= \frac{a_0}{\omega}\sin(\omega t), \\ u(t) &= \frac{a_0}{\omega^2}[1 - \cos(\omega t)], \end{aligned} \tag{11}$$

or a sine-wave acceleration excitation $\ddot{u}(t) = a_0 \sin(\omega t)$ leading to

$$\dot{u}(t) = \frac{a_0}{\omega}[1 - \cos(\omega t)],$$
$$u(t) = \frac{a_0}{\omega^2}[1 - \frac{1}{\omega}\sin(\omega t)]. \quad (12)$$

These functions are shown in Figure 11.

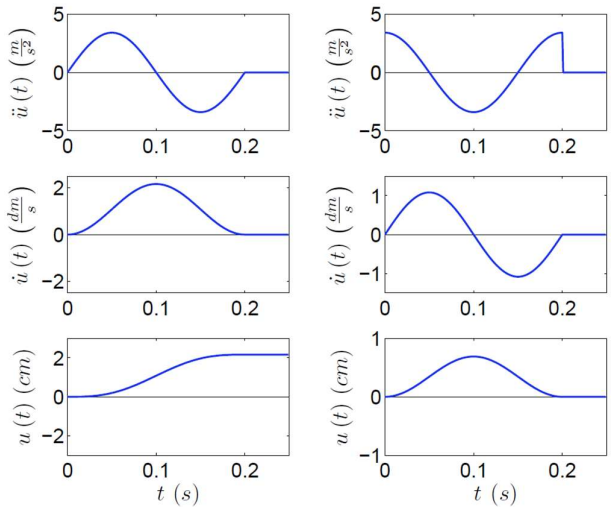

Figure 11. Sine- (left) and cosine-wave (right) acceleration excitation with the corresponding velocity and position functions.

The shaking table system (Quanser ST-III) has the total gait of 10.8 cm in both directions, it can reach a velocity of 2.58 m/s and an acceleration of $3.21g$ with the load-mass roughly corresponding to our heaviest samples. The experiments are carried out so that the two blocks of the same slenderness are put on top of the shaking table and excited at the same time with exactly the same acceleration function, as can be seen in Figure 12.

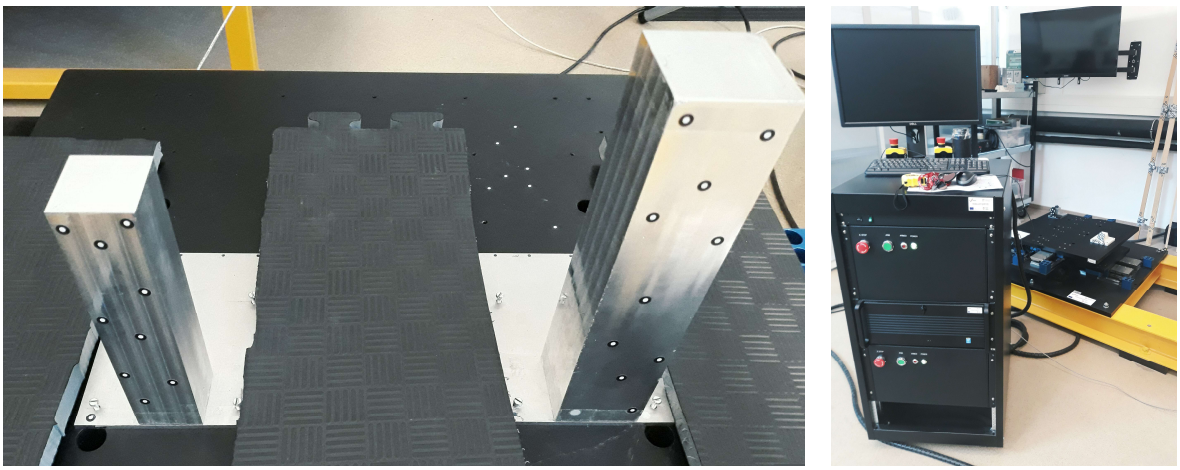

Figure 12. Two blocks of the same slenderness ratio but different size (left) on the shaking table system Quanser ST-III (right).

In each experiment the displacement function actually performed by the shaking table slightly differs from the input displacement function, owing to the inertia of the table and the samples. The displacement is

measured by a linear encoder with one million counts per meter each 0.002 seconds. These results are numerically differentiated with respect to time twice (using the mid-point rule) to check for the 'real' amplitude and frequency of the acceleration function of the table. Furthermore, the acceleration is measured by a biaxial accelerometer embedded in the shaking table system each 0.002 seconds.

The results obtained from post-processing the encoder measurement and from accelerometers measurement has shown to be close to the input values given to the shaking table. For this reason, the experimental results in the rest of this work are presented with respect to the input amplitude and acceleration function.

5 Experimental validation of the algorithm for sine-wave acceleration

The set of four blocks - two bulky blocks with slenderness ratio $\frac{h}{b} = 2.25$ and two slender blocks with slenderness ratio $\frac{h}{b} = 4.5$ - subjected to a sine-wave acceleration function is chosen for experimental validation. The acceleration function is input via a single sine-wave displacement function added to a linear displacement function (12), which satisfies the condition of zero initial velocity of the shaking table, as described in the previous section. The sine-wave excitation described in Section 4.2 is the only one chosen in the experimental analysis because it is much more suitable for testing sensitivity to overturning upon variation of the restitution coefficient (see Section 3.2).

The experiments are performed for each acceleration amplitude starting from the highest acceleration frequency and after each experiment resulting in stable rocking the frequency is lowered. This is repeated until overturning is reached. The experiments close to the boundary between overturning and not-overturning regions are repeated at least three times and the outcome has proven to be repeatable.

5.1 Slender blocks $\frac{h}{b} = 4.5$

The experimentally obtained results for both slender blocks B6M and B6L are shown in Figure 13, along with the simulation results with the average parameter k for each size of the block. These experiments strongly validate the numerically obtained overturning conditions with the restitution coefficient as reported in [24] based on the free rocking tests.

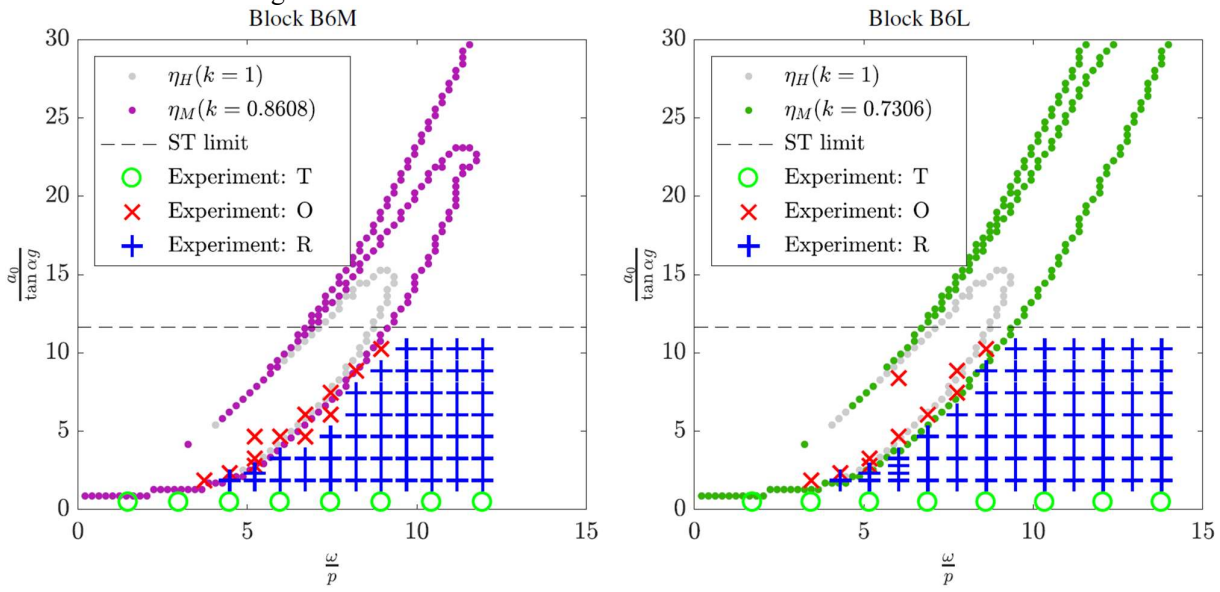

Figure 13. Stability graph due to a single sine wave for blocks B6M and B6L with $\frac{h}{b} = 4.5$ *and average parameter k for each size (T - translation, O - overturning, R - rocking).*

The shaking table system limit is declared as $3.21g$ but, even before reaching the limit, the actual acceleration output starts to resemble a double constant function more than a single sine-function. This

prevents us from checking the overturning conditions for the amplitudes of acceleration functions larger than cca $25\frac{m}{s^2} \approx 2.55g$ (black dashed line labelled as ST limit in Figures 13-16).

In Figure 14 the experimental results are also compared to the simulation results with the parameter k taken as the exact value obtained for that specific block in the previous free-rocking study [24] ($k = 0.8241$ for B6M, $k = 0.7214$ for B6L). The boundary between overturning and non-overturning regions has now somewhat changed - specifically, the overturning area is noticeably larger for the smaller block, but for the acceleration range tested, the experimental results compare equally well with the simulation results.

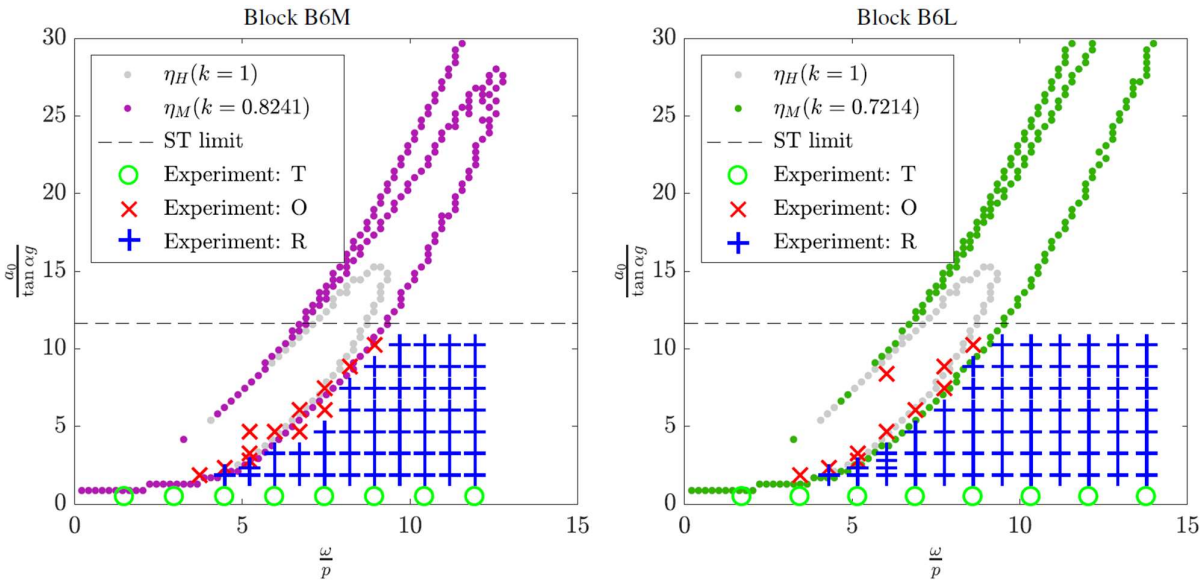

Figure 14. Stability graph due to a single sine wave for blocks B6M and B6L with $h/b = 4.5$ and exact parameter k for each block (T - translation, O - overturning, R - rocking).

5.2 Bulky blocks $\frac{h}{b} = 2.25$

The experimentally obtained results for both bulky blocks B3M and B3L are shown in Figure 15 along with the simulation results with the average restitution for each size from [24] taken into account. The experimental results strongly validate the simulation results in case of the larger block B3L. However, the smaller block B3M overturns in the experiments in the area where the simulations show that stable rocking should occur.

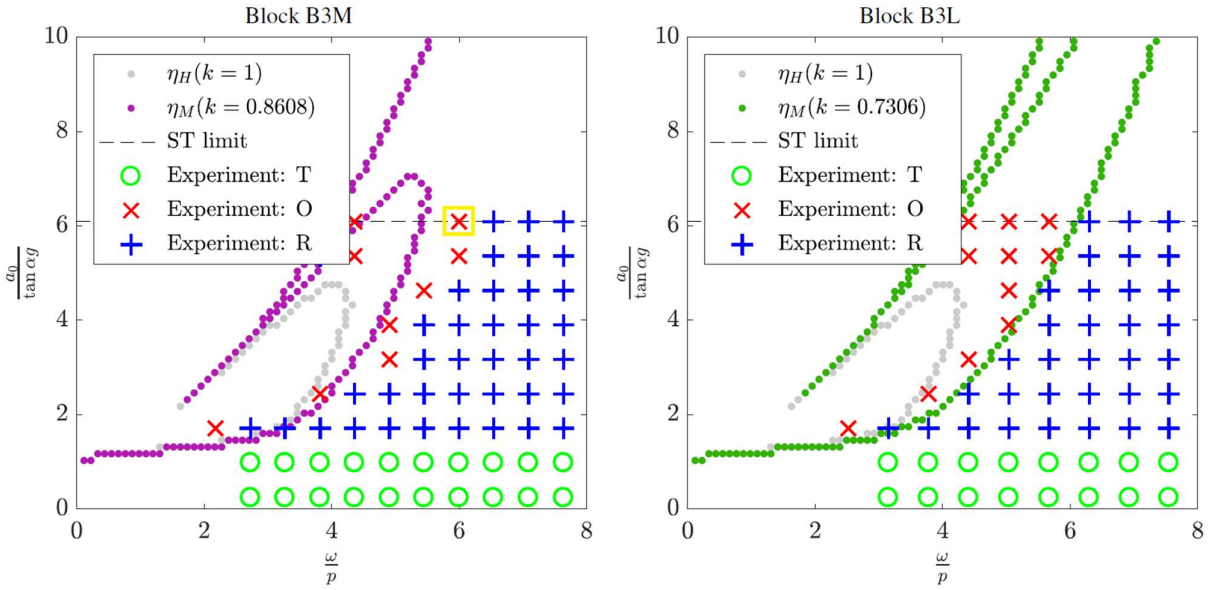

Figure 15. Stability graph due to a single sine wave for blocks B3M and B3L with $\frac{h}{b} = 2.25$ *and average parameter k for each size (T - translation, O - overturning, R - rocking).*

In Figure 16 the experimental results are again compared to the simulation results with the exact value of the parameter k for each block from the free-rocking study in [24] ($k = 0.7595$ for B3M, $k = 0.7259$ for B3L). The overturning area for block B3M is now substantially larger and such a simulation agrees with the experimental results much better.

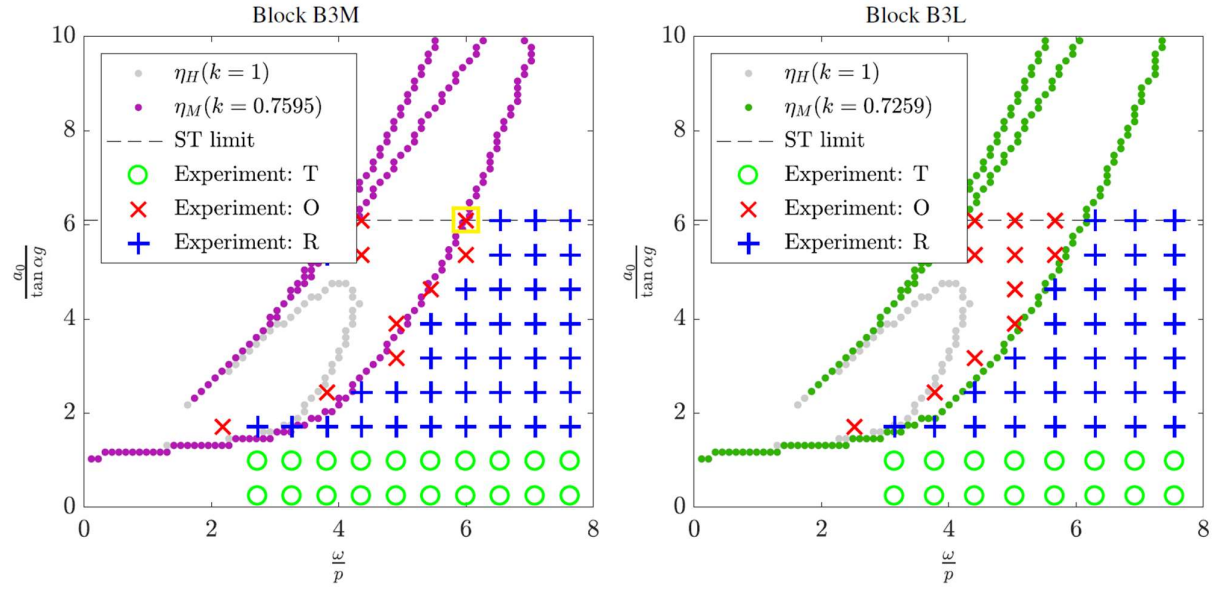

Figure 16. Stability graph due to a single sine wave for blocks B3M and B3L with $\frac{h}{b} = 2.25$ *and exact parameter k for each block (T - translation, O - overturning, R - rocking).*

The sensitivity of the outcome of rocking behaviour (overturning/stable rocking) to small changes in parameter k (thus, in coefficient of restitution) are most obvious if two rotation time-histories of the same block subject to the same base excitation but with different values of parameter k are compared. This is presented in Figure 17 for block B3M subject to a single sine wave excitation with $\frac{\omega}{p} = 6$ and $\frac{a_0}{\mathrm{g}\tan\alpha} = 6.1$ with parameter k equal

to 0.8608 (corresponding to the yellow square in Figure 15) and 0.7595 (corresponding to the yellow square in Figure 16).

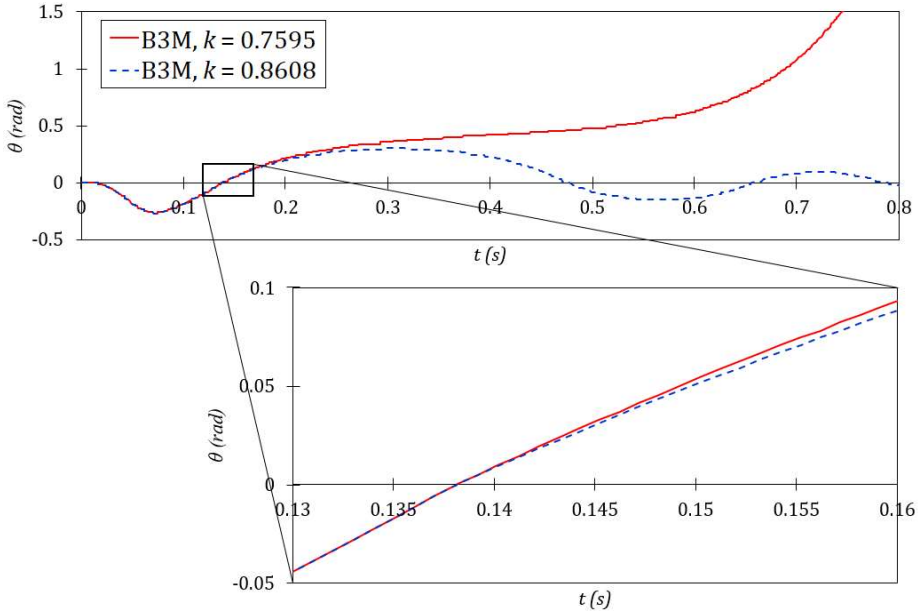

Figure 17. Rotation time-histories for block B3M with parameter k taken as average parameter for size M (blue line) and exact value for block B3M (red line).

Decrease in parameter k results in an increase in coefficient of restitution, thus less energy is lost at the impact just before 0.14 seconds of motion (Figure 17). Such variation in parameter k for block B3M describes a 2.3 mm shift in position of the resultant contact impulse, but it is clearly enough to cause different behaviour after that. In this case, such a shift represents the distinction between block rocking in a stable manner and overturning, which is a critical outcome.

6 Discussion and conclusions

A numerical procedure to obtain overturning conditions for a single rigid block rocking on top of a rigid base, without sliding or jumping, due to a single harmonic wave excitation acceleration is developed and validated against experiments. The code involves an impact detection procedure, and takes into account energy loss during each impact of the block with the base via a restitution coefficient. Both the well-known Housner's restitution coefficient [3], and a recently reported modified restitution coefficient [22], [23] are analysed for their predictive power as stability estimates.

The actual point of impact, needed in the latter, is taken from a free rocking series of tests in [24]. A series of controlled experiments with aluminium blocks on a shaking table subjected to a single sine-wave acceleration function is designed and carried out. The experiments are conducted for two bulky blocks (slenderness $\frac{h}{b} = 2.25$) and two slender blocks (slenderness $\frac{h}{b} = 4.5$) of different sizes. The experimental validation once again proves that Housner's restitution formula is overly liberal and should be avoided in practical use. The modified formula [22], [23] is clearly a better fit to describe real energy loss during rocking, and is strongly encouraged if the position of the impact impulse may be appropriately estimated. In this work this has been performed in conjunction with the free rocking tests conducted earlier.

The simulation involving larger blocks and the restitution coefficient [22], [23] with the additional parameter obtained in this way agree with the experiment very nicely, in contrast with the results using the original Housner's restitution, which is particularly visible for the bulky block. The simulation involving smaller blocks is less precise but still supportive of the use of the modified restitution formula. However, stability graphs for smaller blocks produced numerically by using both the average parameter k obtained for a

given size and the exact parameter k obtained for the analysed block from the free-rocking study result in significantly different overturning areas. When these numerically obtained stability graphs are validated against experimental data, it is clear that the overturning area should be based on the exact value of parameter k for smaller blocks, while it is accurate enough to use the average parameter k for larger blocks. The experimentally obtained cases of overturning which are still outside of the numerically obtained overturning area (after including the exact value of parameter k) show that the method to estimate the impact position should be improved and extended to even smaller blocks, which is what we plan to address in our future work.

Acknowledgements

The results presented in this work have been obtained within the research project *Configuration-dependent approximation in non-linear finite-element analysis of structures* financially supported by the Croatian Science Foundation under contract No. HRZZ-IP-11-2013-1631. The laboratory equipment used in this research is purchased within the project *Research Infrastructure for University of Rijeka Campus (RISK)* founded by the European Fund for Regional Development.

References

[1] N. Makris, "A half-century of rocking isloation," *Earthquakes Struct.*, vol. 7, no. 6, pp. 1187–1221, 2014.
[2] L. Dihoru, A. Crewe, C. Taylor, and T. Horgan, "Shaking Table Experimental Programme," 2011.
[3] G. W. Housner, "The behavior of inverted pendulum structures during earthquakes," *Bull. Seismol. Soc. Am.*, vol. 53, no. 2, pp. 403–417, 1963.
[4] J. Zhang and N. Makris, "Rocking Response of Free-Standing Blocks under Cycloidal Pulses," *J. Eng. Mech.*, vol. 127, no. 5, pp. 473–483, 2001.
[5] N. Makris and Y. Roussos, "Response and Overturning of Equipment under Horizontal Pulse-Type Motions," Berkeley, 1998.
[6] N. Makris and J. Zhang, "Rocking Response and Overturning of Anchored Equipment under Seismic Excitations," Berkeley, 1999.
[7] P. D. Spanos and A.-S. Koh, "Rocking of rigid blocks due to harmonic shaking," *J. Eng. Mech.*, vol. 110, no. 11, pp. 1627–1642, 1985.
[8] T. Winkler, K. Meguro, and F. Yamazaki, "Response of rigid body assemblies to dynamic excitation," *Earthq. Eng. Struct. Dyn.*, vol. 24, no. 10, pp. 1389–1408, 1995.
[9] E. Dimitrakopoulos and M. DeJong, "Overturning of Retrofitted Rocking Structures under Pulse-Type Excitations," *J. Eng. Mech.*, vol. 138, no. 8, pp. 936–972, 2012.
[10] B. Shi, A. Anooshehpoor, Y. Zeng, and J. N. Brune, "Rocking and overturning of precariously balanced rocks by earthquakes," *Bull. Seismol. Soc. Am.*, vol. 86, no. 5, pp. 1364–1371, 1996.
[11] N. Makris and D. Konstantinidis, "The Rocking Spectrum and the Shortcomings of Design Guidlines," Berkeley, 2001.
[12] R. N. Iyengar and C. S. Manohar, "Rocking response of rectangular rigid blocks under random noise base excitations," *Int. J. Non. Linear. Mech.*, vol. 26, no. 6, pp. 885–892, 1991.
[13] P. R. Lipscombe and S. Pellegrino, "Free Rocking of Prismatic Blocks," *J. Eng. Mech.*, vol. 119, no. 7, pp. 1387–1410, Jul. 1993, doi: 10.1061/(ASCE)0733-9399(1993)119:7(1387).
[14] F. Prieto, P. B. Lourenço, and C. S. Oliveira, "Impulsive Dirac-delta forces in the rocking motion," *Earthq. Eng. Struct. Dyn.*, vol. 33, no. 7, pp. 839–857, 2004, doi: 10.1002/eqe.381.
[15] S. Lagomarsino, "Seismic assessment of rocking masonry structures," *Bull. Earthq. Eng.*, vol. 13, no. 1, pp. 97–128, 2015, doi: 10.1007/s10518-014-9609-x.
[16] F. Peña, F. Prieto, P. B. Lourenço, A. Campos Costa, and J. V. Lemos, "On the dynamics of rocking motion of single rigid-block structures," *Earthq. Eng. Struct. Dyn.*, vol. 36, no. 15, pp. 2383–2399, Dec. 2007, doi: 10.1002/eqe.739.
[17] C. Casapulla and A. Maione, "Free damped vibrations of rocking rigid blocks as uniformly accelerated motions," *Int. J. Struct. Stab. Dyn.*, vol. 17, no. 6, Aug. 2017, doi: 10.1142/S0219455417500584.
[18] C. Casapulla and A. Maione, "Critical response of free-standing rocking blocks to the intense phase of an earthquake," *Int. Rev. Civ. Eng.*, vol. 8, no. 1, pp. 1–10, 2017, doi: 10.15866/irece.v8i1.11024.

[19] K. Kojima, K. Fujita, and I. Takewaki, "Critical double impulse input and bound of earthquake input energy to building structure," 2015, doi: 10.3389/fbuil.2015.00005.

[20] K. Nabeshima, R. Taniguchi, K. Kojima, and I. Takewaki, "Closed-Form Overturning Limit of Rigid Block under Critical Near-Fault Ground Motions," *Front. Built Env.*, vol. 2, p. 9, 2016, doi: 10.3389/fbuil.2016.00009.

[21] C. Casapulla, "On the Resonance Conditions of Rigid Rocking Blocks," *Int. J. Eng. Technol.*, vol. 7, no. 2, pp. 760–771, 2015.

[22] D. Kalliontzis, S. Sritharan, and A. Schultz, "Improved Coefficient of Restitution Estimation for Free Rocking Members," *J. Struct. Eng.*, vol. 142, no. 12, 2016.

[23] M. N. Chatzis, M. Garcia Espinosa, and A. W. Smyth, "Examining the Energy Loss in the Inverted Pendulum Model for Rocking Bodies," *J. Eng. Mech.*, vol. 143, no. 5, 2017.

[24] N. Čeh, G. Jelenić, and N. Bićanić, "Analysis of restitution in rocking of single rigid blocks," *Acta Mech.*, vol. 229, no. 11, pp. 4623–4642, Nov. 2018, doi: 10.1007/s00707-018-2246-8.

[25] G. Vlachakis, C. Colombo, A. I. Giouvanidis, A. Mehrotra, N. Savalle, and P. B. Lourenço, "An equivalent viscous damping proposal for block-based rocking models," in *COMPDYN Proceedings*, 2021, vol. 2021-June, doi: 10.7712/120121.8520.18975.

[26] M. Mennitti, S. Maiorano, and S. Aversa, "IOP Conference Series: Earth and Environmental Science Effect of rear walls on the rocking response of rock blocks under seismic excitations," doi: 10.1088/1755-1315/833/1/012085.

[27] Y. Liu, J. Páez Chávez, P. Brzeski, and P. Perlikowski, "Dynamical response of a rocking rigid block," *Chaos*, vol. 31, no. 7, 2021, doi: 10.1063/5.0040962.

[28] D. Kalliontzis and M. Nazari, "Unbonded Post-tensioned Precast Concrete Walls With Rocking Connections: Modeling Approaches and Impact Damping," *Front. Built Environ.*, vol. 7, p. 21, Apr. 2021, doi: 10.3389/fbuil.2021.638509.

[29] M. F. Vassiliou, K. R. Mackie, and B. Stojadinović, "A finite element model for seismic response analysis of deformable rocking frames," *Earthq. Eng. Struct. Dyn.*, vol. 46, no. 3, pp. 447–466, Mar. 2017, doi: 10.1002/eqe.2799.

[30] N. M. Newmark, "A method of computation for structural dynamics," *J. Eng. Mech. Div.*, vol. 85, no. 3, pp. 67–94, 1959.